Indian J Phys (June 2018) 92(6):695–703
https://doi.org/10.1007/s12648-017-1153-5

ORIGINAL PAPER

Analysis and characterization of Cu_2CdSnS_4 quaternary alloy nanostructures deposited on GaN

A A Odeh[1], Y Al-Douri[2,3]*, M Ameri[4] and A Bouhemadou[5]

[1]Khawarizmi International College, 68297 Al Ain, UAE

[2]Nanotechnology and Catalysis Research Center (NANOCAT), University of Malaya, 50603 Kuala Lumpur, Malaysia

[3]Physics Department, Faculty of Science, University of Sidi-Bel-Abbes, 22000 Sidi-Bel-Abbès, Algeria

[4]Laboratoire Physico-Chimie des Matériaux Avancés (LPCMA), Université Djilali Liabès de Sidi Bel-Abbès, 22000 Sidi Bel-Abbès, Algeria

[5]Laboratory for Developing New Materials and Their Characterization, University of Setif 1, 19000 Setif, Algeria

Received: 08 July 2017 / Accepted: 18 October 2017 / Published online: 23 December 2017

Abstract: Through using spin coating technique, Cu_2CdSnS_4 (CCTS) quaternary alloy nanostructures were successfully deposited on GaN substrate using a wide range of spin coating speeds; 1500, 2000, 2500, 3000 and 3500 RPM at annealing temperature 300 °C. The optical properties were investigated through UV–vis which revealed the changing of energy band gap as the spin coating speed increases, in addition, to verify specific models of refractive index and optical dielectric constant. The structural properties were studied by X-ray diffraction which indicated that the number and intensity of the peaks were changed as the spin coating speed changes. The morphological and topographical studies of CCTS were elaborated by field emission-scanning electron microscopy and atomic force microscopy. The obtained results suggest that CCTS nanostructures deposited on GaN substrate are very suitable for optoelectronic applications, that are in accordance with the available theoretical and experimental data.

Keywords: Quaternary alloy; GaN; Spin coating; Band gap

PACS Nos.: 61.66.Dk; 77.84.Bw; 81.15.-z; 42.70.Qs

1. Introduction

Copper-based quaternary I_2–II–IV–VI_4 chalcogenide semiconductors have attracted intensive interest due to their composition of abundant elements that have high optical and structural characteristics useful for many applications such as photovoltaics and sensors. Copper indium gallium selenide (CIGSe) is a tetrahedrally bonded semiconductor with the chalcopyrite crystal structure. $Cu(In,Ga)Se_2$ (CIGSe) chalcopyrite has been synthesized by selenization in the vacuum, the structural properties of CIGSe are strongly affected by increasing the selenization temperature up to 550 °C [1]. Due to limited resources of indium and gallium, the cost of these materials remains high. Other quaternary and quinternary alloys semiconductors have been tested such as $CuTaInSe_3$ [2], $ACdGeAs_2$ [3], Cu_2FeSnS_4 [4, 5], $InGaZnO_4$ [6], $Cu_2Zn_{1-x}Cd_xSnS_4$ [7, 8], $Cu_{1.85}(Cd_xZn_{1-x})_{1.1}SnS_{4.1}$ [9]. The Cu_2ZnSnS_4 (CZTS) with kesterite structure has recently attracted much interest as prospective photovoltaic materials. These direct band gap p-type semiconductors contain only abundant and non-toxic elements [10–12].

Cu_2CdSnS_4 (CCTS) is a copper-based quaternary chalcopyrite semiconductor with an optimal band gap (around 1.5 eV) well suited for using in solar cells. It is worth mentioning, the shape and size of nanostructures may affect the performance and function of the optoelectronics. A limited number of works has explored CCTS and a number of methods has been used to synthesize it such as radio-frequency magnetron sputtering [13], solvothermal [14], electrosynthesis [15], sequential electrodeposition [16] and ultrasonic spray pyrolysis [17]. Using ultrasonic in synthesizing CCTS quaternary alloy nanostructures, via

*Corresponding author, E-mail: yaldouri@yahoo.com

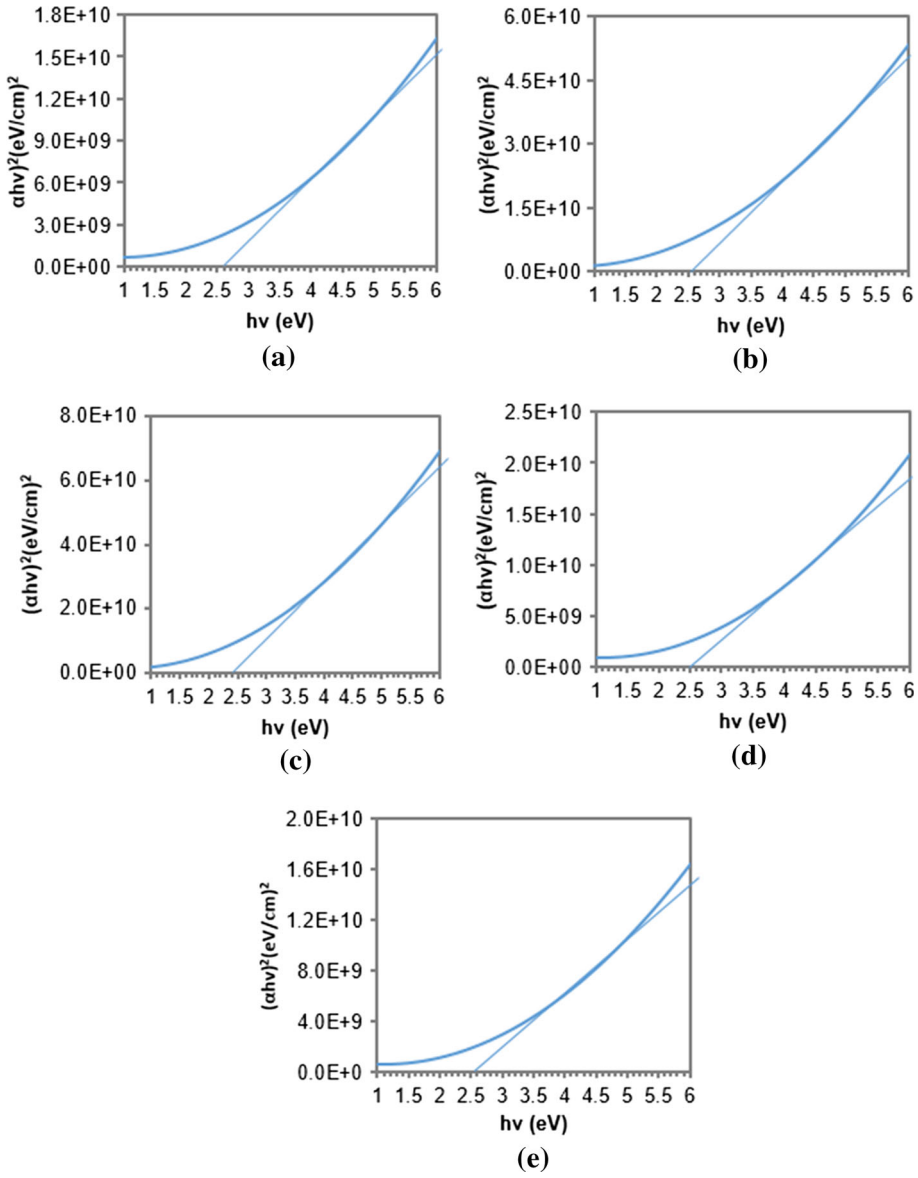

Fig. 1 Fitted $(\alpha h\nu)^2$ versus hν of CCTS quaternary alloy nanostructures deposited on GaN substrates using spin coating speed at **(a)** 1500, **(b)** 2000, **(c)** 2500, **(d)** 3000 and **(e)** 3500 RPM

spin coating technique, introduces more peaks, where the crystallite size increases under high annealing temperature [18]. CCTS quaternary alloy nanostructures have been synthesized and deposited on n-Si substrates via spin coating technique with an annealing temperature of 300 °C at different copper concentrations; 0.2, 0.4, 0.6, 0.8 and 1 M. Lattice constants are decreased as copper concentration increases. Also, energy band gap is changing as Cu concentration increases [19]. Cu_2CdSnS_4 single crystalline nanowires have been prepared via a simple nanoconfined solvothermal method, the porous anodic aluminum oxide is used for the formation of single crystalline Cu_2CdSnS_4 nanowires. The prepared nanowires are uniform with plan (112) and the band gap is found to be 1.52 eV [14].

Gallium nitride (GaN), is a III–V semiconductor that gained significant attention due to its electrical and optical properties as well as chemical stability and biocompatibility over other semiconductors. GaN constitutes the material group of choice when considering solid-state lighting [20, 21]. It has a wide direct band gap of 3.4 eV at room temperature and it is used in many applications such as high power laser, light-emitting diodes (LED) and detectors [22–25]. Hexagonal wurtzite structure of GaN with orientation (002) was deposited on Si substrate by spin coating technique, whereas the topography studies have showed a crack free thin film with uniform and dense grains of GaN were formed [26, 27]. Triangular GaN nano/micro scale needles grown on nickel coated c-plane sapphire substrate with a cross-section forms a triangle that reduces along the growth direction, thus, these needles have wurtzite structure with lattice constants a = 3.19 Å and c = 5.18 Å [28]. Herein, CCTS quaternary alloy

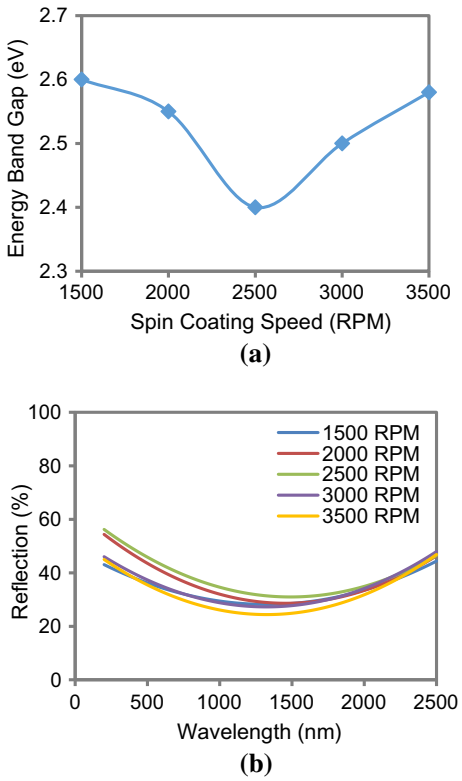

Fig. 2 **(a)** UV–vis plots of energy band gap of CCTS quaternary alloy nanostructures deposited on GaN substrates as a function of the spin coating speed. **(b)** Fitted reflection (%) spectra of CCTS quaternary alloy nanostructures deposited on GaN substrates using different spin coating speeds

nanostructures were synthesized and then deposited, using different spin coating speeds; 1500, 2000, 2500, 3000 and 3500 RPM on GaN substrate at annealing temperature 300 °C. The optical, structural, morphological and topographical properties of quaternary alloy were investigated thoroughly.

2. Experimental details

2.1. Synthesis of CCTS solution

All chemicals and solvents were purchased from Sigma-Aldrich (USA, http://www.sigmaaldrich.com). The precursor solutions of CCTS quaternary alloy nanostructures were prepared from copper (II) chloride dihydrate (0.6 M), cadmium (II) chloride dihydrate (0.8 M), tin (II) chloride dihydrate (0.8 M), thiourea (0.8 M), 2-methoxyethanol and monoethanolamine. The solvent and stabilizer were 2-methoxyethanol and monoethanolamine, respectively. The molar ratios of Cu, Cd, Sn and S in the solution were 2:1:1:4. The specified molar concentrations of the precursors were identified using the following equations;

$$Molarity\,(M) = \frac{n}{V} \tag{1}$$

$$n = \frac{m(\mathrm{g})}{M_m(\mathrm{g/mol})} \tag{2}$$

where n is moles of solute, V is liters of solution, m is mass (g) and M_m is molecular mass (g/mol). The precursors were mixed using a magnetic stirrer for 3 h (1500 RPM) at 50 °C to dissolve the metals completely, which forms a yellow and transparent solution. It is worth mentioning here, the molarity of copper (0.6 M) was chosen based on a previous study [19].

2.2. Solution deposition using spin-coating technique

Spin coating technique was used to deposit the CCTS solution onto GaN (0001) substrates. A few drops of the resulted solution were dropped, using a plastic dropper, on the GaN substrate. A spin coater (Laurell WS-400B, USA) was used at five different spin coating speeds; 1500, 2000, 2500, 3000 and 3500 RPM for 30 s to deposit the solution

Table 1 Measured energy band gaps of CCTS quaternary alloy nanostructures deposited on GaN substrates using UV–vis at different spin coating speeds

Speed (RPM)	Eg (eV) (nm)	n	ε_∞
1500	2.7 1.265[a] 1.25[b]	3.18[d] 3.00[e] 2.82[f]	10.11[d] 9.00[e] 7.95[f]
2000	2.55	3.14[d] 2.97[e] 2.80[f]	9.85[d] 8.82[e] 7.84[f]
2500	2.4 1.65[c]	3.11[d] 2.95[e] 2.78[f]	9.67[d] 8.70[e] 7.72[f]
3000	2.5	3.08[d] 2.92[e] 2.77[f]	9.48[d] 8.52[e] 7.67[f]
3500	2.6	3.05[d] 2.89[e] 2.75[f]	9.30[d] 8.35[e] 7.56[f]

[a]Reference [18] Theo

[b]Reference [19] Theo.

[c]Reference [8] Exp.

[d]Reference [32]

[e]Reference [33]

[f]Reference [34]

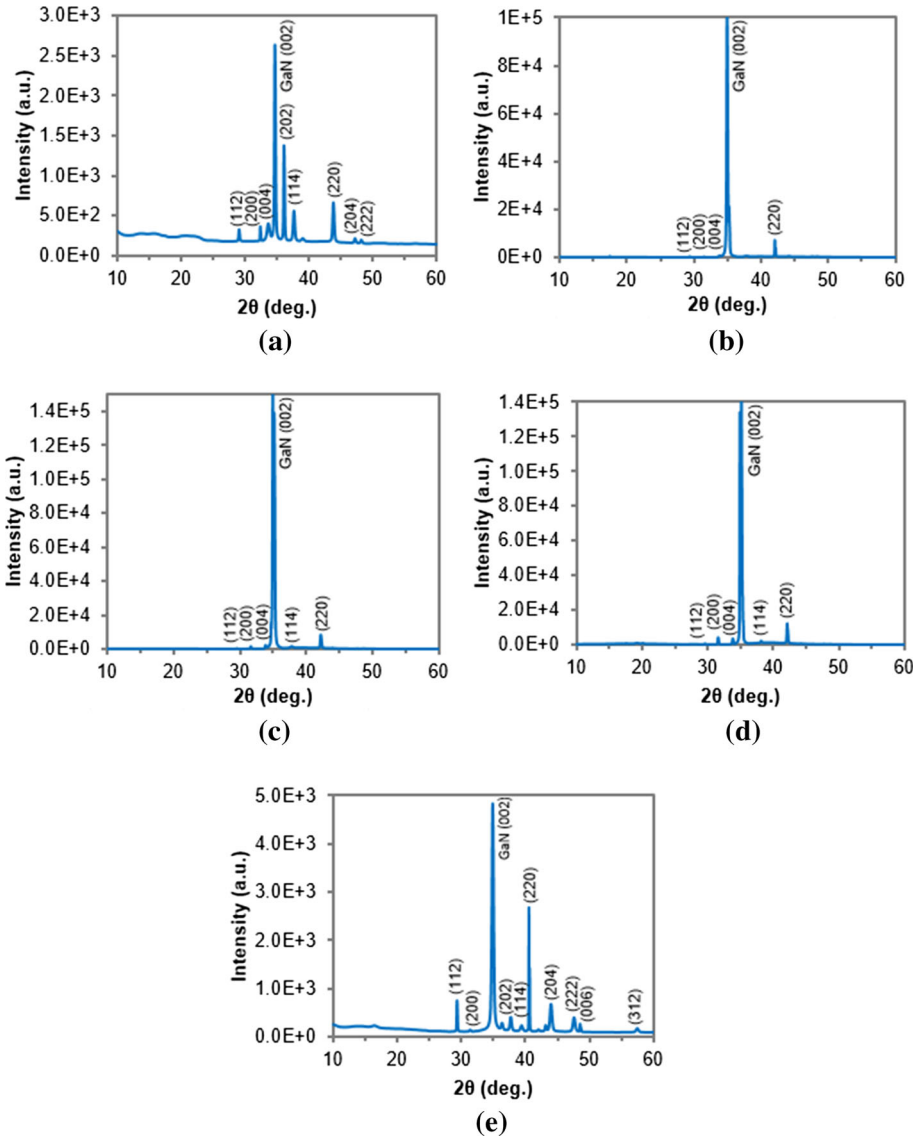

Fig. 3 XRD patterns of CCTS quaternary alloy nanostructures deposited on GaN substrate using spin coating speed at **(a)** 1500, **(b)** 2000, **(c)** 2500, **(d)** 3000 and **(e)** 3500 RPM

on five different substrates, followed by drying on the hot plate at 80 °C for 1 min. The spin coating and drying processes were repeated 8 times to obtain a uniform nanostructure layer with a proper thickness at the top of the substrate. The resulted substrates were annealed at 300 °C for 1 h under the flow of N_2 gas to keep the deposited nanostructure coherent and then cooled to room temperature.

The optical properties of CCTS have been tested using UV–vis spectrometer (Perkin Elmer Lambda 35, USA). The reflection spectra were recorded over the wavelength range 200–2500 nm and the energy band gap has been identified. Also, the structural properties have been investigated via X-ray diffractometer (Bruker D2 PHASER, Germany), which record the intensity as a function of Bragg's angle in the 2θ range from 10° to 60° using Cu kα ($\lambda = 1.5406$ Å). The major diffraction peaks have been recorded and attributed to the corresponding planes. The topography was characterized by Atomic Force Microscopy (AFM) (SPA 400, Seiko Instruments Inc., Japan) with a scanning area of 10 μm × 10 μm and a scanning rate of 1 Hz, whereas, the surface morphology was investigated using field emission-scanning electron microscopy (FE-SEM) (Nova NanoSEM 450, USA) with a magnification factor of ×10,000.

3. Results and discussion

3.1. Optical properties

The reflection versus wavelength measurements was performed at room temperature using UV–vis spectroscopy at the range; 200–2500 nm to investigate the reflection

spectra. According to Tauc model for direct band gap semiconductors [29], the energy band gap of CCTS quaternary alloy nanostructures can be estimated using [18]:

$$(\alpha hv)^2 = A(hv - E_g) \quad (3)$$

where α is the absorption coefficient, A is a constant, E_g is the energy band gap, v is an incident photon frequency and h is the Planck's constant. The energy band gap was estimated from absorption spectra $(\alpha hv)^2$ versus hv by extrapolating the straight line portion of the curve to zero absorption coefficient as shown in Fig. 1. The E_g at 1500 RPM was 2.7 eV, then it is decreased to 2.55 eV with increasing the speed to 2000 RPM, followed by another decreasing to 2.4 eV at 2500 RPM. Energy gap increased again to 2.5 eV with increasing the speed to 3000 RPM and ended up at 2.6 eV with increasing the speed to 3500 RPM, these results are illustrated in Fig. 2a and Table 1. It is worth mentioning, the energy band gap in this study is higher than other studies that used silicon as a substrate due to using GaN as a substrate. The correlation of energy band gap and thin film thickness with spin coating speed is directly, however, the behavior of energy band gap and thickness in this study could be related to some defects on GaN substrate surface due to cleaning the substrate with sulfuric acid along with other materials before solution deposition. Also, other factors may arise such as contamination of spin coater and/or hot plate. As depicted in Fig. 2b, it is observed that the highest reflection was at 2500 RPM followed by 2000, 1500, and 3000 RPM, whereas, the lowest reflection was at 3500 RPM. This promotes the use of 3500 RPM as a first choice followed by 3000 RPM since the lowest reflectance is considered to be the highest absorbance.

The refractive index n is a significant physical parameter in microscopic atomic interactions. Theoretically, the refractive index is related to the density and the local polarizability of these entities [30]. Many simple relationships between refractive index n and the energy gap E_g have been attempted [31–38]. Here, various relationships between n and E_g have been reviewed in order to validate the current work. As suggested by Ravindra et al. [31], the band gap and the high-frequency refractive index, present a linear relationship:

$$n = \alpha + \beta E_g, \quad (4)$$

where $\alpha = 4.048$ and $\beta = -0.62\ \text{eV}^{-1}$.

Inspired by simple physics of light refraction and dispersion, Herve and Vandamme [32] have proposed an empirical relation as:

$$n = \sqrt{1 + \left(\frac{A}{E_g + B}\right)^2} \quad (5)$$

where $A = 13.6$ eV and $B = 3.4$ eV.

Ghosh et al. [33] had taken a different approach by considering the band structural and quantum-dielectric formulations of Penn [39] and Van Vechten [40]. Introducing, A (contribution from the valence electrons) and B (constant additive to the lowest band gap E_g), the expression was written as:

$$n^2 - 1 = A/(E_g + B)^2, \quad (6)$$

Table 2 The structural parameters of CCTS quaternary alloy nanostructures deposited on GaN substrates using XRD at different spin coating speeds

Speed (RPM)	2θ	Particle size (D) (nm)	full width at half maximum (FWHM)	Miller indices (hkl)	Interplaner distance (d) Å	Lattice constants (a and c) Å	Strain (ε)	Dislocation density (δ) (10^{14} lines/m^2)	Number of crystallites particles/area (N) ($\times 10^{15}$)	Thickness (t) (nm)
1500	29.52	54.5	0.1574	112	3.07	a = 5.31, c = 10.63 a = 5.17, c = 10.35[a] a = 5.23, c = 10.46[b]	0.04	3.37	0.408	66
2000	29.71	87.1	0.0984	112	3.05	a = 5.26, c = 10.54	0.023	1.32	0.0707	46.8
2500	29.12	87.2	0.0984	112	3.03	a = 5.24, c = 10.48 a = 5.55, c = 11.95[c]	0.023	1.31	0.092	61.1
3000	29.45	72.6	0.1181	112	3.03	a = 5.23, c = 10.47	0.028	1.9	0.255	98
3500	29.28	89.3	0.096	112	3.05	a = 5.27, c = 10.55	0.023	1.25	0.156	11.1

[a]Reference [18] Theo.

[b]Reference [19] Theo.

[c]Reference [8] Exp.

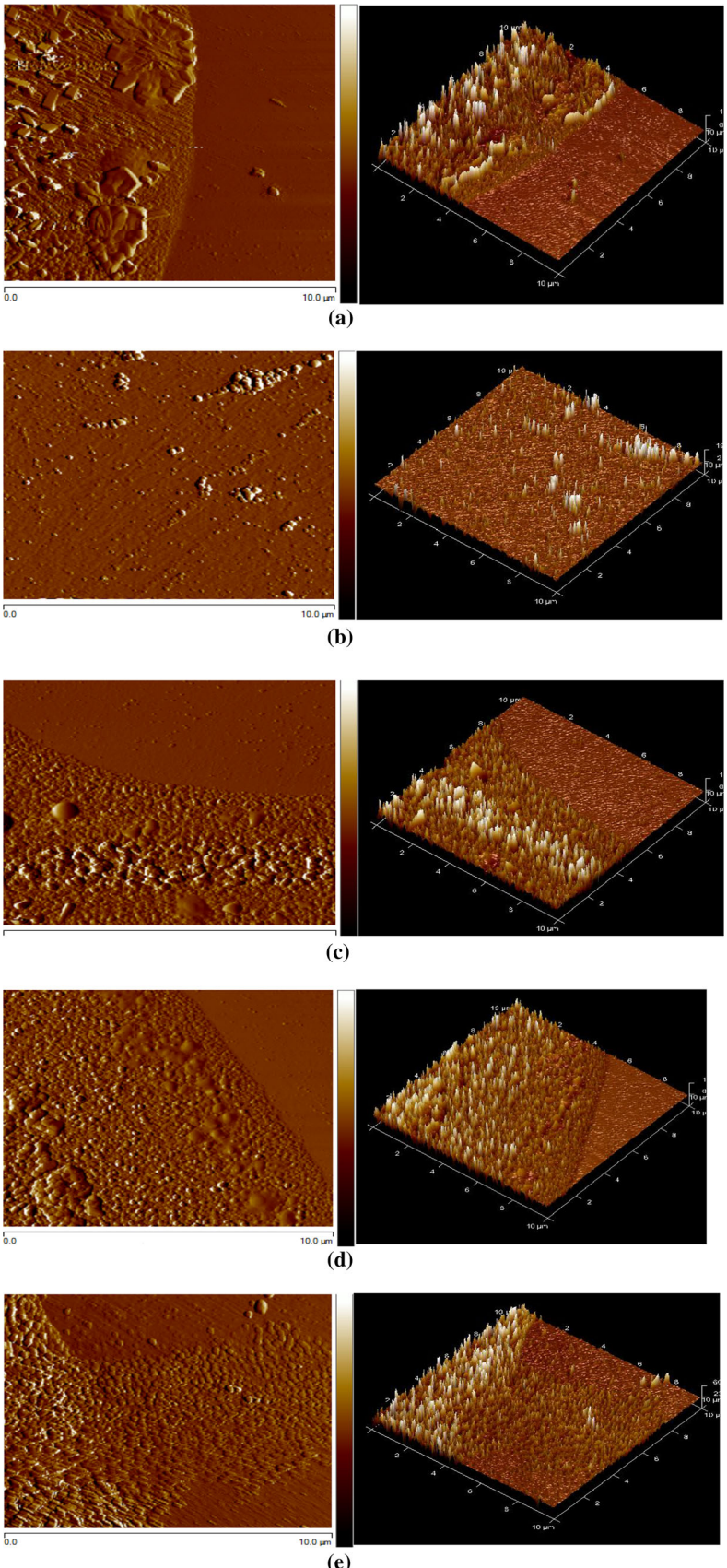

Fig. 4 3D and 2D AFM images of CCTS quaternary alloy nanostructures deposited on GaN substrates using spin coating speed at **(a)** 1500, **(b)** 2000, **(c)** 2500, **(d)** 3000 and **(e)** 3500 RPM

Table 3 The roughness and depth of CCTS quaternary alloy nanostructures deposited on GaN substrates using AFM at different spin coating speeds

Speed (RPM)	Roughness (nm)	Depth (nm)
1500	38.3	175.75
2000	1.68	28.19
2500	15.7	140.21
3000	17.7	74.6
3500	23.6	70.21

where $A = 25E_g + 212$, $B = 0.21E_g + 4.25$ and $(E_g + B)$ refers to an appropriate average energy gap of the material. Thus, these three models for variation of n with energy gap have been tried. In addition, the calculated values of the optical dielectric constant (ε_∞) were obtained using the relation $\varepsilon_\infty = n^2$ [41]. The calculated refractive index and optical dielectric constant are given in Table 1. This is showing that the Ghosh et al. model is an appropriate model for studies.

3.2. Structural properties

XRD pattern provides information about the structural properties, content and size of crystalline structures. The CCTS quaternary alloy nanostructures were investigated by XRD as shown in Fig. 3. After studying the patterns at 1500 RPM, nine major diffraction peaks appeared at $2\theta = 29.52°$, 32.41°, 33.64°, 34.56°, 36.45°, 37.12°, 43.72°, 47.91° and 48.33°, which were attributed to 112, 200, 004, 002, 202, 114, 220, 204 and 222 planes, respectively. At 2000 RPM, five peaks appeared at $2\theta = 29.71°$, 31.41°, 33.82°, 34.88° and 42.13°, which were attributed to 112, 200, 004, 002 and 220. Patterns at 2500 RPM shows an existence of six peaks at $2\theta = 29.12°$, 31.62°, 33.84°, 34.69°, 37.77° and 42.15°, which were attributed to 112, 200, 004, 002, 114 and 220 planes, respectively. Whereas, the CCTS nanostructures deposited at 3000 RPM have six major diffraction peaks appeared at $2\theta = 29.45°$, 31.53°, 33.76°, 34.86°, 38.08° and 42.20°, which were attributed to 112, 200, 004, 002, 114 and 220 planes, respectively. Lastly, XRD patterns at 3500 RPM indicated an existence of ten peaks at $2\theta = 29.28°$, 31.32°, 34.83°, 37.65°, 39.85°, 41.98°, 43.92°, 47.51°, 48.49° and 57.37°, which were attributed to 112, 200, 002, 202, 114, 220, 204, 222, 006 and 312 planes, respectively. It is worth mentioning, the peak that falls between 34° and 35° belongs to GaN (002) due to using GaN as a substrate instead of silicon. Also, there are more peaks at 1500 and 3500 RPM than other speeds, especially at 3500 RPM. On the other hand, the peaks at 1500 and 3500 RPM have less intensity than peaks in other speeds. All resulting peaks were matched with the tetragonal stannite structure of CCTS corresponding to the standard (ICDD PDF2008, 00-029-0537). The lattice constants a and c along with other structural parameters were calculated from XRD data as given in Table 2

$$\frac{1}{d^2} = \frac{h^2 + k^2}{a^2} + \frac{l^2}{c^2} \tag{7}$$

where hkl is Miller indices, a and c are lattice constants. The inter-planer distance (d) was calculated using Bragg's law [42];

$$d = \frac{n\lambda}{2sin(\theta)} \tag{8}$$

The crystallite size (D) was calculated using Scherrer's formula [43];

$$D = \frac{k\lambda}{\beta cos(\theta)} \tag{9}$$

where k is a constant, which equals 0.94, and β is the full width at half maximum (FWHM) of the diffraction peak in radian. The dislocation density (δ), strain (ε) and the number of crystallites per unit area (N) are also given in Table 2. These parameters are calculated using;

$$\delta = \frac{1}{D^2} \tag{10}$$

$$\varepsilon = \frac{\beta cos\theta}{4} \tag{11}$$

$$N = \frac{t}{D^3} \tag{12}$$

where t is the thickness. As given in Table 2, the calculated lattice constants are in accordance with available data [8, 18, 19, 44], moreover, both of them are decreased with increasing the speed linearly until reaching 3500 RPM where they are going up again.

3.3. Topographical and morphological studies

The surface topography of CCTS quaternary alloy nanostructures has been characterized. Figure 4 shows 2-D and 3-D images with an area of 10 μm × 10 μm at 1 Hz scan rate. The surface roughness is related to the quaternary alloy diffusion type, substrate type, annealing temperature and spin coating speed. As displayed in Table 3, the measured roughness was 38.3 nm at 1500 RPM, it is dropped rapidly to 1.68 nm with increasing the speed to 2000 RPM. It is increased again to 15.7 nm at 2500 RPM followed by another increasing until it reaches 17.7 nm at 3000 RPM and finally ended up with 23.6 nm at 3500

RPM. The depth of CCTS nanostructures was identified also in the same table. The depth was the highest value of 170.75 nm at 1500 RPM followed by a large drop value of 28.19 nm at 2000 RPM. It is increased again to 140.21 nm with increasing the speed to 2500 RPM then dropped back again to 74.6 nm at 3000 RPM and continued to decreasing until it reaches 70.21 nm at 3500 RPM.

Morphology of nanostructures depends on material composition, synthesis method, crystal structure and

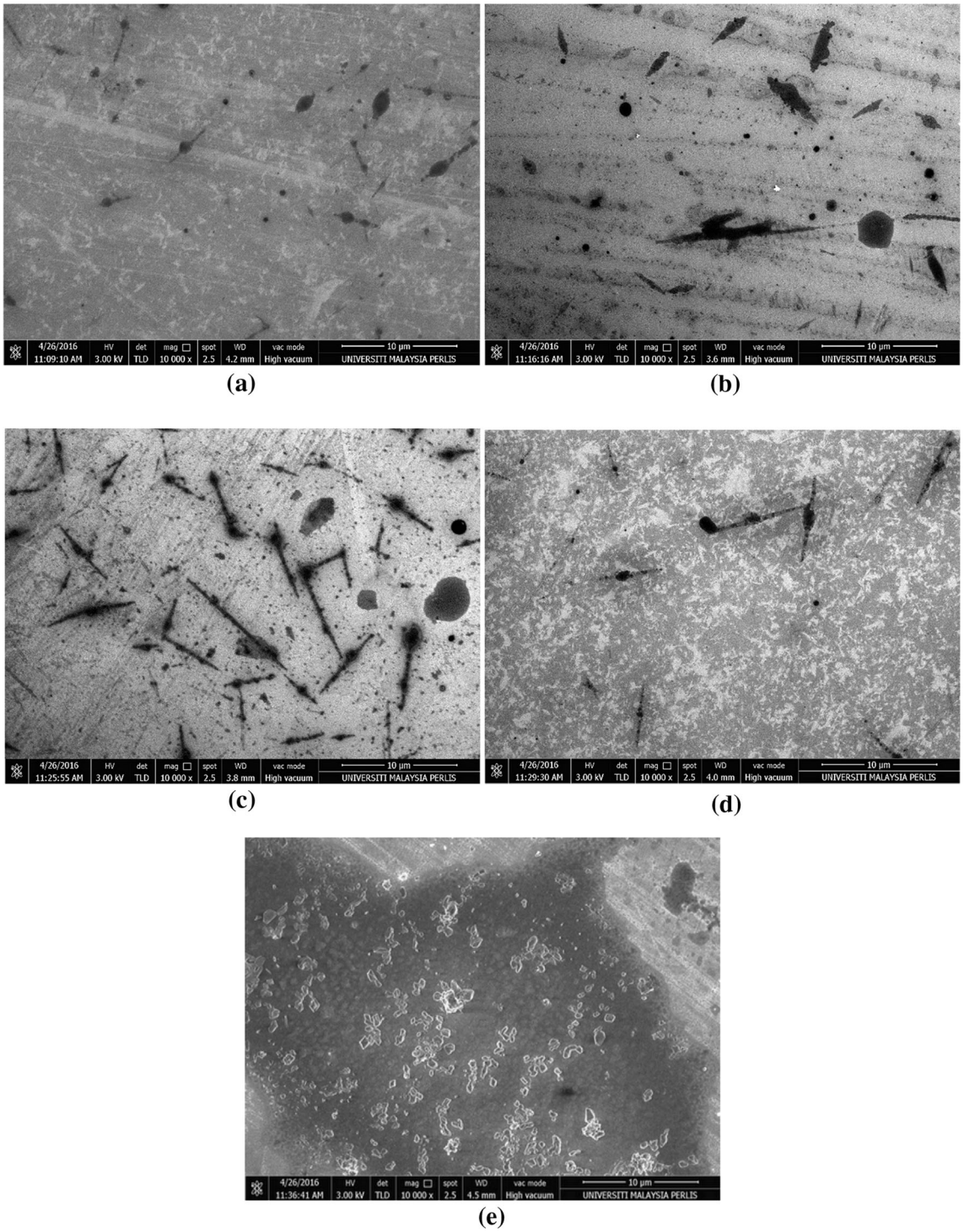

Fig. 5 FE-SEM images of CCTS quaternary alloy nanostructures deposited on GaN substrates using spin coating speed at **(a)** 1500, **(b)** 2000, **(c)** 2500, **(d)** 3000 and **(e)** 3500 RPM

manufacturing method. The FE-SEM images are shown in Fig. 5 and depicted the surface morphology of CCTS quaternary alloy nanostructures at different spin coating speeds with a magnification factor of ×10,000. A closer look at the images shows that the best image was at a speed; 3500 RPM.

4. Conclusions

This work involved the synthesis of CCTS quaternary alloy nanostructures using multiple spin coating speeds; 1500, 2000, 2500, 3000 and 3500 RPM and deposited on GaN substrate. The results have shown that the speed increases from 1500 RPM to 3500 RPM has led to decreasing the energy band gap from 2.7 to 2.4 and then increasing again to 2.6 eV. The reflection spectra at 3500 RPM was the lowest which means that the absorbance is the highest. The largest number of peaks are existed at 3500 RPM furthermore, the intensity of these peaks are the smallest compared with their counterparts in other speeds. Also, the crystallite size is the smallest at 3500 RPM. It is worth mentioning, the morphology of CCTS nanostructures was the best at 3500 RPM. Ghosh et al. model is recommended at 3500 RPM. Of these facts, using 3500 RPM as a spin coating speed as well as GaN as a substrate will lead to enhancing the characteristics of CCTS nanostructures for optoelectronics.

Compliance with ethical standards

Conflict of interest The authors declare that they have no conflict of interest.

References

[1] F B Dejene *Curr. Appl. Phys.* **10** 36 (2010)
[2] P Grima-Gallardo, M Munoz, S Duran, G E Delgado, M Quintero and J Ruiz *Mater. Res. Bull.* **42** 2067 (2007)
[3] S Azama, S A Khan and S Goumri-Said *Mater. Res. Bull.* **70** 847 (2015)
[4] C Rincón, M Quintero, E Moreno, Ch Power, E Quintero, J A Henao, M A Macías, G E Delgado, R Tovar and M Morocoima *Solid State Commun.* **151** 947 (2011)
[5] K Mokurala, P Bhargava and S Mallick *Mater. Chem. Phys.* **147** 371 (2014)
[6] M-C Wu, K-C Hsiao and H-C Lu *Mater. Chem. Phys.* **162** 386 (2015)
[7] G Nkwusi, I Leinemann, J Raudoja, V Mikli, E Karba and M Altosaar *Superlattices Microstruct,* **98** 400 (2016)
[8] A S Ibraheam, Y Al-Douri, U Hashim, D Prakash, K D Verma and M Ameri *J. Mater. Sci.* **51** 6876 (2016)
[9] M Pilvet, M Kauk-Kuusik, M Altosaar, M Grossberg, M Danilson, K Timmo, A Mere and V Mikli *Thin Solid Films* **582** 180 (2015)
[10] R Bacewicz, J Antonowicz, S Podsiadło and S Schorr *Solid State Commun.* **177** 54 (2014)
[11] T A Oliveira, J Coutinho and V J B Torres *Thin Solid Films* **535** 311 (2013)
[12] S G Lee, J Kim, H S Woo, Y Jo, A I Inamdar, S M Pawar, H S Kim, W Jung and H S Im *Curr. Appl. Phys.* **14** 254 (2014)
[13] L Meng, Y Li, B Yao, Z-H Ding, G Yang, R-J Liu, R Deng and L Liu *J. Phys. D Appl. Phys.* **48** 445105 (2015)
[14] L Shi, C Wu and J Ding *J. Alloys Compd.* **683** 46 (2016)
[15] S M Pawara, B S Pawara, A V Moholkara, D S Choia, J H Yunc, J H Moona, S S Kolekarb and J H Kima *Electrochim. Acta* **55** 4057 (2010)
[16] X He, H Shen, J Pi, C Zhang and Y Hao *J. Mater. Sci. Mater. Electron.* **24** 4578 (2013)
[17] S Kermadi, S Sali, F Ait Ameur, L Zougar, M Boumaour, A Toumiat, N N Melnik, D W Hewak *Mater. Chem. Phys.* **169** 96 (2015)
[18] A A Odeh, Y Al-Douri, R M Ayub and A S Ibraheam *J. Alloys Compd.* **686** 883 (2016)
[19] A A Odeh, Y Al-Douri, R M Ayub, M Ameri, A Bouhemadou, D Prakash and K D Verma *Appl. Phys. A* **122** 888 (2016)
[20] M A Borysiewicz, M Wzorek, K Gołaszewska, R Kruszka, K D Pagowska and E Kaminska *Mater. Sci. Eng. B* **200** 93 (2015)
[21] S J Wilkins, T Paskova and A Ivanisevic *Appl. Surf. Sci.* **327** 498 (2015)
[22] G Grecoa, F Iucolanob and F Roccaforte *Appl. Surf. Sci.* **383** 324 (2016)
[23] H Li, C Xue, H Zhuang, J Chen, Z Yang, L Qin, Y Huang and D Zhang *Mater. Chem. Phys.* **109** 249 (2008)
[24] A Ariff, N Zainal and Z Hassan *Superlattices Microstruct.* **97** 193 (2016)
[25] B Liua, L Hub, C Tangb, L Liua, S Li and J Qia *Mater. Sci. Eng. B* **176** 805 (2011)
[26] A Cruz-López, A Manzo-Robledo, O Vázquez-Cuchillo, R Zanella, R Gómez, J Santoyo-Salazar, A Campos-Badillo *Mater. Sci. Semicond. Process.* **30** 435 (2015)
[27] C Y Fong, S S Ng, F K Yam, H Abu Hassan and Z Hassan *Mater. Sci. Semicond. Process.* **17** 63 (2014)
[28] M Kumar, A Kumar, S B Thapa, S Christiansen and R Singh *Mater. Sci. Eng. B* **186** 89 (2014)
[29] A A Ahmad *J. Mater. Sci. Mater. Electron.* 28 1695 (2017)
[30] N M Balzaretti and J A H da Jornad *Solid State Commun.* 99 943 (1996)
[31] N M Ravindra, S Auluck and V K Srivastava *Phys. Status Solidi (B)* **93** k155 (1979)
[32] P J L Herve and L K J Vandamme *J. Appl. Phys.* **77** 5476 (1995)
[33] D K Ghosh, L K Samanta and G C Bhar *Infrared Phys.* **24** 43 (1984)
[34] Y Al-Douri, H Khachai and R Khenata *Mater. Sci. Semicond. Process.* **39** 276 (2015)
[35] Y Al-Douri, U Hashim, R Khenata, A H Reshak, M Ameri, A Bouhemadou, A Rahim Ruslinda and M K Md Arshad *Solar Energy* **115** 33 (2015)
[36] Y Al-Douri *Mater. Chem. Phys.* **82** 49 (2003)
[37] Y Al-Douri, Y P Feng and A C H Huan *Solid State Commun.* **148** 521 (2008)
[38] Y Al-Douri, A H Reshak, H Baaziz, Z Charifi, R Khenata, S Ahmad, U Hashim *Solar Energy* **84** 1979 (2010)
[39] D R Penn *Phys. Rev.* **128** 2093 (1962)
[40] J A Van Vechten *Phys. Rev.* **182** 891 (1969)
[41] G A Samara *Phys. Rev.* B **27** 349 (1983)
[42] Y Al-Douri, Q Khasawneh, S Kiwan, U Hashim, S B Abd Hamid, A H Reshak, A Bouhemadou, M Ameri and R Khenata *Energy Convers. Manage.* **82** 238 (2014)
[43] Y Al-Douri and A H Reshak *Optik* **126** 5109 (2015)
[44] A A Odeh, Y Al-Douri, C H Voon, R M Ayub, S C B Gopinath, R A Odeh, M Ameri and A Bouhemadou *Microchim. Acta* **184** (2017) 2211